

⁵ Chung, P. M., "Chemical Reaction in a Turbulent Flow Field with Uniform Velocity Gradient," *The Physics of Fluids*, Vol. 13, No. 5, May 1970, pp. 1153-1165.

⁶ Chung, P. M., "A Simplified Statistical Model of Turbulent, Chemically Reacting Shear Flows," *AIAA Journal*, Vol. 7, No. 10, Oct. 1969, pp. 1982-1991.

⁷ Chung, P. M., "Chemically Reacting Non-equilibrium Boundary Layers," *Advances in Heat Transfer*, Vol. 2, Academic Press, New York, 1965, Chap. 2.

⁸ Chung, P. M., "On the Development of Diffusion Flame in Homologous Turbulent Shear Flows," *AIAA Paper 70-722*, 1970, San Diego, Calif.

Fluid Dynamics in a Large Arterial Bifurcation

CZESLAW M. RODKIEWICZ* AND DARREL H. HOWELL†
University of Alberta, Edmonton, Canada

Nomenclature

- d = unstressed internal diameter of side branch
- D = unstressed internal diameter of main branch
- L = approximate length of entry region
- Q_d = flow rate in side branch
- Q_D = flow rate in main branch
- Re = Reynolds number, Eq. (1)
- R_o = unstressed internal radius of main branch
- t = time variable
- u = longitudinal coordinate of velocity
- U = average longitudinal velocity
- U' = fluctuating component of longitudinal velocity
- α = unsteadiness parameter, Eq. (2)
- β = ratio of branch diameters
- γ = mass-flow ratio
- θ = angle of branching
- λ = normalized velocity fluctuation, Eq. (3)
- ν = kinematic fluid viscosity
- ω = pulse rate

Introduction

THE present work on the blood flow in a large arterial bifurcation was suggested by N. R. Kuchar whose Ph.D. thesis¹ and recent paper on blood flow devices² gave the necessary theoretical background. The primary objective is to investigate the effect of varying the significant dimensionless parameters on the manner in which the flow divides at a bifurcation.

The heart produces a periodic or pulsatile flow on the arterial side of the circulatory system. The amplitude of the flow pulse is largest in the aorta and becomes gradually smaller as the system branches. The arterial vessels are subjected to higher pressure and pressure variation, and they are thicker and contain more elastin than the venous system. Despite the extra strength and elasticity of the arterial walls,

Received August 12, 1970; revision received July 8, 1971. The authors wish to thank N. R. Kuchar of the General Electric Space Sciences Laboratory in Philadelphia, and R. D. Laurenson of the Department of Anatomy of the University of Alberta, for their helpful suggestions during the course of the present work; P. Quoc, for his very efficient assistance in the construction of the apparatus during the summer of 1969; T. Gates and B. Romanko for their assistance in conducting the experiments during the summer of 1970. This research was done in connection with the National Research Council of Canada Grant NRC A-4198.

Index categories: Space Medicine (Including Weightlessness, Radiation Effects, Psychology, etc.); Spacecraft Habitability and Life Support Systems.

* Research Director.

† Graduate Student.

it seems likely that a system under the continual wear and tear of a pulsatile flow would be subject to many disorders. Such is the case, arterial disease being a very great problem. One of the disorders is the atherosclerosis.³ It refers to the build up of fatty and/or fibrous plaques which occlude the vessel and destroy the elasticity of its wall.

Experimental Range

Flow in an arterial bifurcation is described by five dimensionless parameters.^{1,2} The first two are the Reynolds number and the unsteadiness parameter, respectively,

$$Re = UD/\nu \quad (1)$$

$$\alpha = D(\omega/\nu)^{1/2} \quad (2)$$

It is now necessary to determine the range of these parameters for the physiological case. To do this, the following data has been selected^{4,5}: a) The relative viscosity of blood with respect to distilled water varies from 3.5-5.4; b) blood density varies from 1.048-1.066 gm/cm³; c) the kinematic viscosity of distilled water equals 0.010027 cm²/sec; d) for an average case, blood flows at a mean velocity of 32 cm/sec through an aorta of 2.1 cm diam; e) human pulse rate varies from 50-100 beats per min; f) the diameter of the human aorta varies from 1.5-2.1 cm. Substitution of these data into Eqs. (1) and (2) yields the following experimental ranges of study: $1300 < Re < 2040$, $6 < \alpha < 15$.

Attinger et al.⁶ show that a Fourier series can be used to approximate periodic blood flow in the cardiovascular system. The first harmonic, a sine wave, has the highest amplitude. We therefore assume that flow from the heart can be approximated as a sinusoidal flow. The normalized velocity fluctuation λ is defined by the following expression

$$\lambda = U'/U \quad (3)$$

where U is the mean velocity and U' is the peak to peak amplitude of the fluctuating component of velocity. Kuchar and Scala² report the physiological range for λ to be $1 < \lambda < 2$.

This work is confined to the case of the side branch off a straight vessel as illustrated in Fig. 1. Consideration of this bifurcation geometry gives rise to two additional dimensionless parameters—the angle between the branches, θ , and the ratio of the branch diameters, $\beta = d/D$. The following ranges of experimental study have been chosen for θ and β : $30^\circ \leq \theta \leq 90^\circ$, $0.20 \leq \beta \leq 0.80$.

Apparatus

Figure 2 gives the schematic of the apparatus. The bifurcations were made of glass. The inlet and outlet to the bifurcation were surgical tubing suspended by twine from a dexion frame. The upstream was approximately 8 ft in length and as straight and horizontal as possible. Kuchar and Ostrach¹ calculated that a length ratio (R_o/L) of 0.193 was necessary to ensure the elimination of end effects. The length ratio of the apparatus was 0.0065. Therefore, the entrance length of the apparatus was more than sufficient for flow stability.

For ease of observation, the internal diameter of the main branch of the experimental model has 1.25 in. Weiting⁷

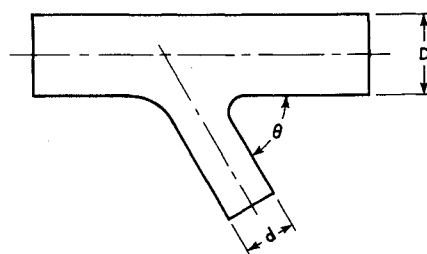


Fig. 1 The experimental bifurcation.

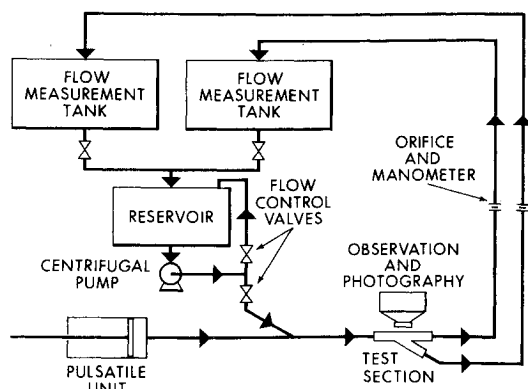


Fig. 2 Schematic of the apparatus.

found that a 36.7% glycerol-aqueous solution was a good hydraulic analogy for blood. The specific gravity of this mixture is 1.10 and the viscosity is 4.5 centipoise. The viscosity falls within the range accepted for human blood and the specific gravity is reasonably close. For the purpose of flow visualization, resin particles were suspended in the blood analogue.

Bell, Davidson, and Scarborough⁸ quote the mean diastolic pressure at the inlet of the aorta as 90 mm Hg. This is equivalent to about 4 ft of blood which was the approximate vertical displacement of the inlet to the flow measurement tanks above the plane of the test section. Flow rates were measured directly by the rate at which the measurement tanks filled.

The sinusoidal flow was obtained by using a centrifugal pump in series with a cam-driven piston cylinder arrangement powered by a variable speed d.c. motor. The experimental fluid was allowed to assume the ambient temperature. Since the building in which the experiments were conducted is air conditioned, the temperature could be assumed constant throughout. Because of the time and financial limitations, no attempt was made to reproduce the experimental results.

Experimental Results

The mass-flow ratio γ was defined as the ratio of the flow rate in the side branch Q_d to the flow rate in the mainline branch Q_D , $\gamma = Q_d/Q_D$. The dependence of γ on α , Re , and λ was examined. Each parameter was varied throughout its range while the other four parameters were held constant.

The mass-flow ratio γ , as a function of the unsteadiness parameter α , and the normalized fluctuating component of velocity λ , is presented in Fig. 3. The Reynolds number was kept constant at $Re = 1630$ and the bifurcation used was defined by the parameters $\beta = 0.75 \text{ in.}/1.25 \text{ in.} = 0.60$ and $\theta = 50^\circ$. The dependence of γ on α was examined for $\lambda = 1.0$,

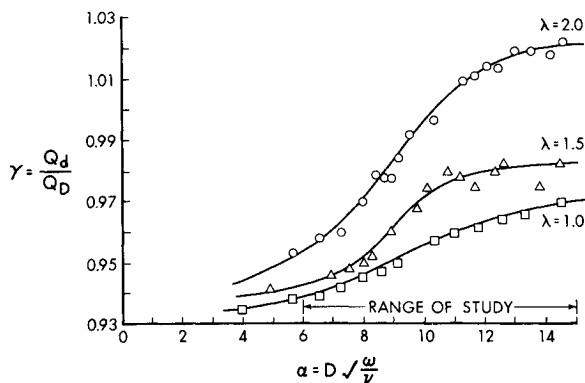


Fig. 3 Mass-flow ratio γ vs unsteadiness parameter α for $\lambda = 1.0, 1.5, 2.0$, $\beta = 0.75/1.25 = 0.60$; $\theta = 50^\circ$; $Re = 1630$.

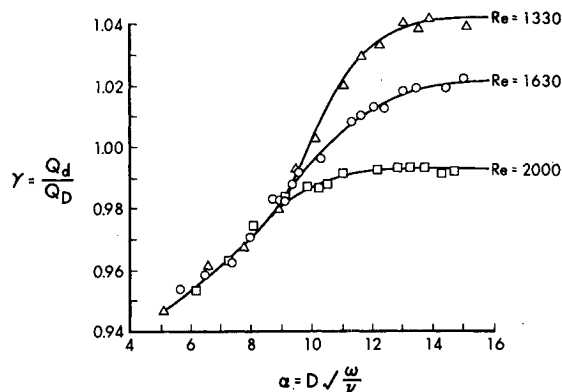


Fig. 4 Mass-flow ratio γ as a function of unsteadiness parameter α and Reynolds number Re , $\beta = 0.75/1.25 = 0.60$; $\theta = 50^\circ$; $\lambda = 2.0$.

1.5, and 2.0. Figure 3 indicates that γ increases as α and λ increase. A possible explanation for the dependence of γ on α stems from the dependence of the velocity profile on the cycle frequency.⁹ Since α is directly proportional to the square root of the frequency, increasing α will flatten the velocity profile. Consequently, as α increases, proportionally more fluid will flow in the area near the outer walls than in the center of the vessel. Since flow in the side branch originates in the area proximal to the main vessel wall, a greater percentage of flow to the side branch results.

Similarly the turbulent flow has flatter velocity profile than has laminar flow.⁹ Mitchell and Schwartz,³ and McDonald,⁹ recognize the existence of turbulent flow in a portion of the flow cycle and observations by the authors corroborate this viewpoint. As λ increases, the magnitude of the maximum instantaneous velocity increases and it follows that the flow is turbulent for a greater portion of the cycle. This would result in a flattened velocity profile for a longer period of time and may be one of the reasons for the increase in γ with increased λ .

The mass-flow ratio γ , as a function of the unsteadiness parameter α and the Reynolds number Re , is presented in Fig. 4. The fluctuating component of the velocity was kept constant at $\lambda = 2.0$. The dependence of γ on α was examined at $Re = 1330, 1630$, and 2000 . Figure 4 indicates that, above a certain threshold of α , γ decreases as the Reynolds number increases.

Summary of the Experimental Results

A generalized summary of the experimental findings of the present work is as follows: a) the mass-flow ratio γ is a function of the unsteadiness parameter α and the normalized velocity fluctuation λ , which increases with increasing α and λ ; b) below a threshold of the unsteadiness parameter, $\alpha = 8.8$, the mass-flow ratio γ is independent of the Reynolds number, Re . Above this threshold value, γ is a function of Re which decreases with an increase in Re .

These results indicate that the heart, activated by an impulse from the brain, can produce a particular pulse rate ω of a given amplitude λ and selected Reynolds number Re so that more blood may be supplied to the preferential area of the human body. For example, on an emergency signal requiring additional blood supply to the area of the head, as much as necessary of blood has to be diverted into the side branch, say $\gamma > 1$. This, for a given Reynolds number, is achieved by the synchronized increase in α and λ .

References

- ¹ Kuchar, N. R. and Ostrach, S., "Flows in the Entrance Regions of Circular Elastic Tubes," FTAS/TR-65-3, June 1965, Case Western Reserve Univ., Cleveland, Ohio.
- ² Kuchar, N. R. and Scala, S. M., "Design of Devices for Optimum Blood Flow," Publ. 68-DE-52, 1968, ASME.

³ Mitchell, J. R. A. and Schwartz, C. J., *Arterial Disease*, Blackwell Scientific Publications, Oxford, 1965.

⁴ Wintrobe, M. M., *Clinical Haematology*, Lea and Febiger, Philadelphia, 1968.

⁵ Tuttle, W. W. and Schottelius, B. A., *Textbook of Physiology*, C. V. Mosby Co., St. Louis, 1965.

⁶ Attinger, E. O., Anné, A., and McDonald, D. A., "Use of Fourier Series for the Analysis of Biological Systems," *Biophysical Journal*, Vol. 6, 1966, p. 291.

⁷ Wieting, D. W., "A Method of Analyzing the Dynamic Flow Characteristics of Prosthetic Heart Valves," 68-WA/BHF-3, 1968, ASME.

⁸ Bell, G., Davidson, J. N., and Scarborough, H., *Textbook of Physiology and Biochemistry*, 6th ed., E. & S. Livingston Ltd., Edinburgh and London, 1965.

⁹ McDonald, D. A., *Blood Flow in Arteries*, Edward Arnold Ltd., London, 1960.

N-Step Conjugate Gradient Minimization Scheme for Nonquadratic Functions

ISAAC FRIED*

Massachusetts Institute of Technology,
Cambridge, Mass.

Introduction

IN a recent report,¹ Jacobson and Oksman describe a new algorithm for function minimization. The novel and most prominent feature of this algorithm is its ability to minimize in $N + 2$ steps not only quadratics but also a larger class of homogeneous functions. In this regard this algorithm may prove superior (as shown experimentally in Ref. 1) to the widely used conjugate direction techniques as adapted to the minimization of nonquadratic functions by Davidon,² Fletcher and Powell,³ and Fletcher and Reeves.⁴ Both the variable metric technique of Davidon and that of Jacobson and Oksman require the storage and updating of an $N \times N$ full or half matrix.

One of the important uses of the minimization scheme is for solving the large algebraic systems generated by the finite element (or any other discretization) method applied to nonlinear problems via a direct search^{5,6} for the minimum. The number of variables may be so large in such cases that the $N \times N$ matrix will no longer fit into the core, and both the variable metric method as well as the method of Jacobson and Oksman may prove to be disadvantageous from the point of view of the programming and execution time. The marked advantage of the conjugate gradient method lies precisely in the avoidance of this matrix.

It is the purpose of this Note to present a new conjugate gradient algorithm which, like that of Jacobson and Oksman, minimizes a larger class of nonquadratic functions in no more than N steps. The algorithm presented here, however, does not require the storage and handling of large full matrices.

Minimization Scheme

Consider the function

$$f = (1/2r)[(x - \xi)^T K (x - \xi)]^r + c \quad (1)$$

where K is an $N \times N$ positive definite matrix. The function f has its minimal value, $f = c$, at $x = \xi$. In the present dis-

cussion it is assumed that c is known and for the sake of simplicity set equal to zero. For $r = 1$ the method of conjugate gradients will minimize f in no more than N steps. As will now be shown, the conjugate gradient algorithm can be modified to insure the convergence of f in N steps not only for $r = 1$ but for any r .

The gradient $g = \nabla f$ of f is written concisely as

$$g = FK(x - \xi) \quad (2)$$

where $F = [(x - \xi)^T K (x - \xi)]^{r-1}$. Starting with x_0 , the gradient $g_0 = \nabla f(x_0)$ is calculated. Then the next x_1 is sought along the search vector $p_0 = g_0$ such that $x_1 = x_0 + \alpha_0 p_0$. Also α_0 is fixed by the condition that f assumes a local minimum with respect to α_0 . The next gradient, g_1 , can be calculated (assuming for the moment that K is given) by $g_1 = F_1(g_0/F_0 + \alpha_0 K p_0)$. As in the quadratic case, the next search direction p_1 is obtained from $p_1 = g_1 + \beta_0 p_0$. The third gradient, g_2 , is given by

$$g_2 = F_2(g_1/F_1 + \alpha_1 K g_1 + \alpha_1 \beta_0 K p_0) \quad (3)$$

and β_0 is obtained from the condition that g_2 is orthogonal to g_0 (and g_1). Hence

$$\beta_0 = -g_0^T K g_1 / g_0^T K g_0 \quad (4)$$

Multiplying

$$g_1 = F_1(g_0/F_0 + \alpha_0 K p_0) \quad (5)$$

by g_1 and g_0 yields $g_1^T K g_0 = g_1^T g_1 / F_1 \alpha_0$ and $g_0^T K g_0 = -g_0^T g_0 / F_0 \alpha_0$, and with these β becomes

$$\beta_0 = g_1^T g_1 F_0 / g_0^T g_0 F_1 \quad (6)$$

The gradient g_2 is now normal to both g_1 and g_0 . Continuing this scheme will generate, as in the quadratic case, a complete set of N orthogonal gradients. Since there can be only N nonzero orthogonal vectors in the N -dimensional space, the $(N + 1)$ th gradient must vanish.

For a general function neither r nor K is known, and the F needed for calculating β in Eq. (6) should be obtained from f and g . Equation (1) readily leads to

$$F_0/F_1 = (f_0/f_1)^{(r-1)/r} \quad (7)$$

Also

$$F_0/F_1 = g_0^T (x_1 - \xi) / g_1^T (x_0 - \xi) \quad (8)$$

and

$$g_0^T \xi = g_0^T x_0 - 2rf_0, \quad g_1^T \xi = g_1^T x_1 - 2rf_1 \quad (9)$$

Then, since $g_1^T (x_0 - x_1) = -g_1^T p_0 \alpha_0 = 0$, introduction of Eq. (9) into Eq. (8) results in

$$F_0/F_1 = (\alpha_0 g_0^T p_0 + 2rf_0) / 2rf_1 \quad (10)$$

The exponent r is obtained from the equation

$$(f_1/f_0)^t = 1 + \alpha_0 p_0^T g_0 / 2f_0 \quad t = 1/r \quad (11)$$

resulting from equating Eqs. (10) and (7). Equation (11) is written concisely as

$$a^t = 1 + bt \quad (12)$$

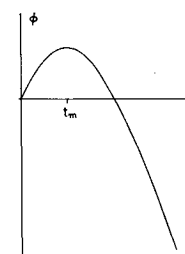


Fig. 1 The function $\phi = -a^t + 1 + bt$. It attains its maximal value at $t = t_m$.

Received June 18, 1971; revision received July 16, 1971. This work was partly supported by the USAF Office of Scientific Research under contract F44620-67-C-0019.

Index category: Structural Static Analysis.

* Post-Doctoral Research Fellow, Department of Aeronautics and Astronautics; now Assistant Professor, Department of Mathematics, Boston University. Associate Member AIAA.